ULTRASONIC IMAGING 22, 39- 54 (2001)

# An Investigation into the Feasibility of Fetal Lung Maturity Prediction Using Statistical Textural Features

K. N. BHANU PRAKASH,[1] A. G. RAMAKRISHNAN, S. SURESH[2] AND TERESA W. P. CHOW[3]

[1]*Biomedical Lab*
*Dept. of Electrical Engg*
*Indian Institute of Science*
*Bangalore, India*
*Email:ramkiag@ee.iisc.ernet.in*

[2]*Fetal Care Research Foundation*
*169, Avvai Shanmugam Road*
*Gopalapuram, Madras, India*

[3]*Dept of Obstetrics and Gynecology*
*University of Malaya*
*Kuala Lumpur, Malaysia*

Fetal lung and liver tissues were examined by ultrasound in 240 subjects during 24 to 38 weeks of gestational age in order to investigate the feasibility of predicting the maturity of the lung from the textural features of sonograms. A region of interest of 64 X 64 pixels is used for extracting textural features. Since the histological properties of the liver are claimed to remain constant with respect to gestational age, features obtained from the lung region are compared with those from liver. Though the mean values of some of the features show a specific trend with respect to gestation age, the variance is too high to guarantee definite prediction of the gestational age. Thus, we restricted our purview to an investigation into the feasibility of fetal lung maturity prediction using statistical textural features. Out of 64 features extracted, those features that are correlated with gestation age and less computationally intensive are selected. The results of our study show that the sonographic features hold some promise in determining whether the fetal lung is mature or immature.

KEY WORDS: Fetal lung; lung maturity; prediction; sonogram; texture; textural features.

## 1. INTRODUCTION

Despite many recent advances in perinatal and neonatal care, respiratory distress syndrome (RDS) remains the major cause for morbidity and mortality. A newborn with RDS has physiologically immature lungs, which cannot support adequate gas exchange without medical intervention. Therefore, assessment of fetal lung maturity is an invaluable adjunct to modern perinatal management. RDS syndrome occurs when surface-active compounds are not present in sufficient quantity for the alveoli to remain open at the end of expiration. The lung collapses and can only be opened, for further gas exchange, by the application of high positive pressure. Normal lung remains open at the end of expiration because surfactants lower surface tension on the alveolar surfaces and allow residual air to remain in the individual alveoli.

The development of fetal lung involves two components: the biochemical component of fetal lung maturation is surfactant production and the anatomic component is the development of airways and alveoli with fibroelastic components. Structural development of lung progresses through three stages.[1] During the *glandular stage* (first 16 weeks), the lobes of


0161-7346/01 $18.00

the lungs become well demarcated and bronchi and bronchiole airway divisions develop. The cells lining the airways are thick and columnar proximally and change to cuboidal peripherally. During the *canalicular stage* (from 16 to 24 weeks), the development of distal airway occurs in the form of respiratory bronchiole branching and vascular proliferation at the end of airways. The cells in these distal airways change from cuboidal proximally to thinner flattened epithelial cells distally. The lungs are not yet capable of respiratory function. During the *alveolar stage* (24 weeks to term), respiratory tissue begins to appear at the ends of the respiratory bronchioles as alveolar sacs and eventually, as small alveoli. During this stage, respiration can occur in a premature newborn, if surfactant production is sufficient to lower the surface tension and maintain open airspace.

Anatomic development of fetal lung seems to be closely related to gestational age (GA), while biochemical maturity can occur as early as 28 weeks or as late as term. Prediction of lung maturity is important in the management of high-risk pregnancies. If the lungs are mature to sustain the newborn with no respiratory support, then prolonging of pregnancy is not required. However, if they are immature, then the risks and costs of prolonging pregnancy may have to be weighed, especially, in settings with limited neonatal support.

Methods for determining fetal lung maturity include estimation of fetal size, gestational age, condition of placenta and biochemical tests on amniotic fluid. Though different properties of surfactants in amniotic fluid have been studied, the lecithin/sphingomyelin ratio (L/S ratio) remains the golden standard. All these tests necessitate amniocentesis, an invasive procedure that carries risks, and on occasion, may be contraindicated. On the other hand, ultrasound is a totally noninvasive investigation procedure. Of course, ultrasound can neither measure any of the biochemical parameters of fetal lung maturity nor can it provide direct histological information about fetal lung development. Experimental evidences support the hypothesis that morphological and biochemical changes alter the diffuse scattering and other propagation properties of fetal lung. Such a change translates to appropriate variations in the textural appearance of sonogram. Sonographically-determined parameters such as fetal biparietal diameter and placental grading have been related to fetal maturity, with an accuracy ranging from 78% to 100%.[2]

In the present study, we explore the possibility of estimating the gestation age using the textural features of the sonogram. Arguments for and against the use of sonographic features for analyzing fetal lung maturity have been extensively debated.[2-10] Based on sonographic studies, Thieme et al[3] conclude that the reflectivity of lung is greater than liver reflectivity during mid–gestation and is equal to liver reflectivity at term in lambs. Lamb was chosen as an experimental model, since it had been extensively used in pulmonary physiology research and since lamb lung is reported to progress through the same stages of development as human lung. Garrett et al[4] state that reflectivity of the human fetal lung is equal to or less than that of liver throughout most of pregnancy but that the relationship reverses in late gestation. Nevertheless, Cayea et al[5] argue that there is no statistically-significant correlation between the sonographic features and the biochemical fetal lung maturity indices, namely the L/S ratio and Phosphatidylglycerol (PG) values. Employing rf signals for characterizing fetal lung and liver tissues, Benson et al[6] observe, from the reflected signals, a spectral shift from a higher frequency range to a lower frequency range as the fetal lung makes the transition from immature to mature state. Feingold et al[2] used densitometer measurements to establish a correlation between lung–liver echogenicity and the L/S ratio. Podobnik et al[7] bring forth a relation between the coefficient of variation of lung-liver echogenicity and the L/S ratio. C arson et al[8,9] have come out with a detailed report about the difficulties in predicting the pulmonary maturity using ultrasound. They also reported that technical factors play an important part in determinations of fetal lung maturity. Sohn et al[10, 11] used liver as a reference organ to standardize the fetal lung changes depending on the gestation. They found that liver was an adequate reference organ, since there was no significant change of the reflection pattern between the different weeks of gestation, while significant changes were registered in the fetal lung. Further in 1992 they analyzed 348 subjects and were able to classify the pulmonary maturity and immaturity. They also said it is possible to determine fetal lung maturity very easily and noninvasively . Christie[12] in his technical report of 1992 has also stated that liver can be considered as a reference organ to analyze pulmonary maturity with gestation age. Hararlick et al[13] had proposed textural features, which were computed from the co-occurrence matrix formed from the image and used it for image classification. These statistical features were used in analysis and classification of the ultrasound images.[15, 16] Keller et al[19] used fractal analysis to segment textural images. Chen et al[17] defined a feature vector based on normalized fractional brownian motion (NFBM) to represent the statistical characteristics of the medical image surfaces. Verhoeven et al[18] applied fractal analysis to parametric imaging of B-mode echograms to detect lesions in echographic images.

Based on the above studies, and the possibility of having a noninvasive determination of lung maturity, we decided to investigate the relevance of new ultrasound image texture parameters in tackling the problem of assessing fetal lung maturation. Further, we also explore the use of liver as a reference in the sonogram-based analysis of lung maturity.

## 2. MATERIALS AND METHODS

Ultrasound examinations were performed using the real time ATL Apogee 800 plus scanner with a 3.5 MHz curvilinear, broad bandwidth transducer probe with the dynamic range set at 55 dB. The overall gain was set at an optimal value to get uniform visibility. The appropriate section was frozen and the image was grabbed. Longitudinal and transverse sections of the fetal thorax and upper abdomen were imaged. The fetal lung and liver were identified in the thoracic and upper abdominal sections, respectively. Care was taken to avoid obvious vascular structures in the liver. The machine settings were optimized to obtain a uniform echo texture. The postprocessing curves were unchanged. The focal zone was always adjusted so that the area of interest was in the focal zone. Data was collected from 240 subjects at various gestation ages from 24 to 38 weeks, at regular intervals of two weeks. The subjects were rigorously followed up throughout the pregnancy and also after delivery. Only the data corresponding to normal pregnancies, also leading to babies with normal pulmonary functions, are included in our analysis. The data with untoward outcomes for the fetus or the mother or both were excluded from the study. The motivation was to obtain the trend of the textural features of the normal fetal lung as a function of the gestation age. Data was collected both at Mediscan Systems, Chennai, India and at the University Hospital in Kuala Lumpur, Malaysia. The images were frozen in the machine and then transferred to videotape. The images were then digitized using the Creative video grabber card. The size of the digitized image is 320 X 240 pixels with a resolution of 29 pixels per centimeter. The histogram of the images was first stretched to have a uniform range of gray values and then equalized. A region of interest of 64 X 64 pixels was used for extracting a number of quantitative parameters related to texture. Figure 3 exhibits samples of the fetal echogram showing liver and lung regions, with the ROI selected. The lung to liver ratio[10-12] of various feature values were studied as possible indices of maturity. The details of the features employed are given in the subsections that follow.

### 2.1 Spatial gray level dependence matrices (SGLDM)

The SGLDM are based on the estimation of second order joint conditional probability density functions, $f(i,j|\,d,\theta)$. Here $f(i,j|\,d,\theta)$ is the probability that a pair of pixels separated by a distance d at an angle $\theta$ have gray levels $i$ and $j$. The angles are quantized to $45^\circ$ intervals. The estimated probability density functions, denoted by, $P(i,j|\, d, \theta)$[13] are defined as,

$$P(i,j\,|d,0) = \#\{((k,l),(m,n)) \in (L_X X L_Y)\ X\ (L_Y X L_X): k = m, |l-n| = d, I(k,l) = i, I(m,n) = j\} \\ /T(d,0) \tag{1}$$

$$P(i,j\,|d,45^\circ) = \#\{((k,l),(m,n)) \in (L_X\ X\ L_Y)\ X\ (L_Y X L_X): (k-m = d,\ l-n = -d) \text{ or } (k-m = -d, \\ l-n = d),\ I(k,l) = i,\ I(m,n) = j\}\ /\ T(d,45^\circ) \tag{2}$$

$$P(i,j\,|\,d,90^\circ) = \#\{((k,l),(m,n)) \in (L_X X L_Y)\,X\,(L_Y X L_X): |k-m| = d, l = n, I(k,l) = i, I(m,n) = j\}\ / \\ T(d,90^\circ) \tag{3}$$

$$P(i,j\,|\,d,135^\circ) = \#\{((k,l),(m,n)) \in (L_X X L_Y)\,X\,(L_Y X L_X):(\,k-m = -d,\ l-n = -d,\ I(k,l) = i, \\ I(m,n) = j\}\ /\ T(d,135^\circ) \tag{4}$$

where # denotes the number of elements in the set, $L_X$ and $L_Y$ are the horizontal and vertical spatial domains, $I(x,y)$ is the image intensity at point $(x,y)$, $T(d,\theta)$ stands for the total number of pixel pairs within the image which have the intersample spacing $d$ and direction angle $\theta$. If a texture is coarse and $d$ is small compared to the sizes of the texture elements, the pairs of points at separation distance $d$ should usually have similar gray values. Conversely, for fine structures the gray levels of points separated by distance $d$ should often be quite different.

Haralick[13] proposed 14 texture measures that can be extracted from the $P(i,j\,|\,d,\theta)$ matrices. In our study, only the following five texture features[14] are computed.

$$\text{Energy: } E[S_\theta(d)] = \sum_{i=0}^{N_G-1}\sum_{j=0}^{N_G-1}[s_\theta(i,j\,|\,d)]^2 \tag{5}$$

$$\text{Entropy: } H[S_\theta(d)] = \sum_{i=0}^{N_G-1}\sum_{j=0}^{N_G-1} s_\theta(i,j\,|\,d)\log s_\theta(i,j\,|\,d) \tag{6}$$

$$\text{Correlation: } C[S_\theta(d)] = \frac{\sum_{i=0}^{N_G-1}\sum_{j=0}^{N_G-1}(i-\mu_x)(j-\mu_y)s_\theta(i,j\,|\,d)}{\sigma_x\sigma_y} \tag{7}$$

$$\text{Inertia: } In[S_\theta(d)] = \sum_{i=0}^{N_G-1}\sum_{j=0}^{N_G-1}(i-j)^2 s_\theta(i,j\,|\,d) \tag{8}$$

Local homogeneity: $$L[S_\theta(d)] = \sum_{i=0}^{N_G-1}\sum_{j=0}^{N_G-1}\frac{1}{1+(i-j)^2}s_\theta(i,j\,|\,d) \tag{9}$$

where $s_\theta(i,j\,|\,d)$ is the $(i,j)^{th}$ element of $S_\theta$ for a specified $d$, $N_G$ is the number of gray levels in the image and

$S_0(d) = P(i,j\,|\,d, 0^0)$; $S_{45}(d) = P(i,j\,|\,d, 45^0)$;

$S_{90}(d) = P(i,j\,|\,d, 90^0)$; *and* $S_{135}(d) = P(i,j\,|\,d, 135^0)$;

$$\mu_x = \sum_{i=0}^{N_G-1} i \sum_{j=0}^{N_G-1} s_\theta(i,j\,|\,d) \tag{10}$$

$$\mu_y = \sum_{j=0}^{N_G-1} j \sum_{i=0}^{N_G-1} s_\theta(i,j\,|\,d) \tag{11}$$

$$\sigma^2{}_x = \sum_{i=0}^{N_G-1}(i-\mu_x)^2 \sum_{j=0}^{N_G-1}[s_\theta(i,j\,|\,d)] \tag{12}$$

$$\sigma^2{}_y = \sum_{j=0}^{N_G-1}(j-\mu_y)^2 \sum_{i=0}^{N_G-1}[s_\theta(i,j\,|\,d)] \tag{13}$$

Each measure is evaluated for values of $d=1$ and $d=2$, and $\theta = 0^0, 45^0, 90^0$ and $135^0$.

## 2.2 The Gray Level Difference Matrix (GLDM)

For any given displacement $\delta = (\Delta x, \Delta y)$, let $I_\delta(x,y) = |I(x,y) - I(x+\Delta x, y+\Delta y)|$ and $f'(i\,|\,\delta)$ be the probability density of $I_\delta(x,y)$. If there are $m$ gray values, this has the form of a $m$-dimensional vector whose $i^{th}$ component is the probability that $I_\delta(x,y)$ will have value $i$. The value of $f'(i\,|\,\delta)$ is obtained from the number of times $I_\delta(x,y)$ occurs for a given $\delta$. Explicitly,

$$f'(i\,/\,\delta) = P(I_\delta(x,y) = i) \tag{14}$$

Four possible forms of the vector $\delta$ are considered: $(0,d)$, $(-d, d)$, $(d, 0)$, and $(-d, -d)$, where $d$ is the interpixel distance. From each of these density functions, five texture features[23] were extracted. They are:

$$\text{Contrast: } CON = \sum_{i=0}^{N_G-1} i^2 f'(i \mid \delta) \tag{15}$$

$$\text{Mean} = \sum_{i=0}^{N_G-1} i f'(i \mid \delta) \tag{16}$$

$$\text{Entropy: } ENT = \sum_{i=0}^{N_G-1} f'(i \mid \delta) \log(f'(i \mid \delta)) \tag{17}$$

$$\text{Inverse difference moment: } IDM = \sum_{i=0}^{N_G-1} \frac{f'(i \mid \delta)}{i^2+1} \tag{18}$$

$$\text{Angular second moment: } ASM = \sum_{i=0}^{N_G-1} [f'(i \mid \delta)]^2 \tag{19}$$

### 2.3 Laws' texture energy measures

Laws' texture energy measures[20] are derived from three vectors, each of length three : $L3$ = (1, 2, 1), $E3$ = (-1, 0, 1) and $S3$ = (-1, 2, -1). These, respectively, represent the operations of local averaging, edge detection and spot detection. If these vectors are convolved with themselves or with one another, we obtain, among others, the following five vectors, each of length five: $L5$ = (1, 4, 6, 4, 1), $S5$ = (-1, 0, 2, 0, -1), $R5$ = (1, -4, 6, -4, 1), $E5$ = (-1, -2, 0, 2, 1) and $W5$ = (-1, 2, 0, -2, 1), which perform local averaging, spot, ripple, edge and wave detection, respectively. The masks used in our analysis are

**$L5^T E5$**

| | | | | |
|---|---|---|---|---|
| -1 | -2 | 0 | 2 | 1 |
| -4 | -8 | 0 | 8 | 4 |
| -6 | -12 | 0 | 12 | 6 |
| -4 | -8 | 0 | 8 | 4 |
| -1 | -2 | 0 | 2 | 1 |

**$L5^T S5$**

| | | | | |
|---|---|---|---|---|
| -1 | 0 | 2 | 0 | -1 |
| -4 | 0 | 8 | 0 | -4 |
| -6 | 0 | 12 | 0 | -6 |
| -4 | 0 | 8 | 0 | -4 |
| -1 | 0 | 2 | 0 | -1 |

The masks were convolved with the image and the entropy of the resulting image was calculated.

### 2.4. Fractal dimension and lacunarity

The above conventional methods measure the coarseness, directionality and energy. However, they do not consider an important characteristic, namely, the granularity. An intensity surface of an ultrasonic image can be viewed as the end result of random walks and a fractional Brownian motion model[17] can be used for its analysis. Fractal dimension and lacunarity are the important features that characterize the roughness and granularity of the fractal surface.

Given a $MXM$ image $I$, the intensity difference vector is defined as $IDV = [id(1),\ id(2),\ldots\ id(s)]$, where $s$ is the maximum possible scale and $id(k)$ is the average of the absolute intensity difference of all pixel pairs with horizontal or vertical distance $k$.

We compute $id(k)$ as

$$id(k) = \frac{\sum_{x=0}^{M-1}\sum_{y=0}^{M-k-1} |I(x,y) - I(x,y+k)| + \sum_{x=0}^{M-k-1}\sum_{y-0}^{M-1} |I(x,y) - I(x+k,y)|}{2M(M-k-1)} \tag{20}$$

and $D = 3 - H$, where $D$ is the fractal dimension. The value of $H$ is obtained by using a least-squares linear regression to estimate the slope of the curve of $id(k)$ versus $k$ in a log-log scale. Given a fractal set $A$, let $P(m)$ be the probability that there are $m$ points within a box of size $L$, centered about an arbitrary point of $A$. We have $\sum_{m=1}^{N} P(m) = 1$, where $N$ is the number of possible points within the box. Lacunarity is then defined as

$$\Lambda = \frac{(M_2 - M^2)}{M^2} \tag{21}$$

where

$$M = \sum_{m=1}^{N} mP(m) \tag{22}$$

and

$$M_2 = \sum_{m=1}^{N} m^2 P(m) \tag{23}$$

## 3. RESULTS AND DISCUSSION

Initially, we planned to predict the gestation age from the values of the various parameters computed. However, the variation of the parameters for each gestation age was too high to give an acceptable level of prediction of the gestation age.[21, 22] Hence, we redefined our aim as one leading to the feasibility of fetal lung maturity prediction using statistical textural features. Out of the 64 features extracted, 15 features were selected that were correlated with gestation age and computationally less intensive. Table 2 shows the correlation between the selected features and gestation age. Various statistics of the features were computed, which

**TABLE 1.** Descriptive statistics of the features.

| Gestation | 24 | 26 | 28 | 30 | 32 | 34 | 36 | 38 |
|---|---|---|---|---|---|---|---|---|
| | | | | | | | | |
| Feature | | | | | | | | |
| Fracdim | | | | | | | | |
| | | | | | | | | |
| Mean | 0.997553 | 0.992803 | 1.000472 | 0.994068 | 0.990264 | 0.994453 | 0.984419 | 0.991721 |
| Standard Error | 0.001746 | 0.002 | 0.003702 | 0.001824 | 0.001616 | 0.001706 | 0.002053 | 0.002398 |
| Sample Variance | 0.000326 | 0.000416 | 0.001412 | 0.000309 | 0.000248 | 0.000285 | 0.000447 | 0.000541 |
| Minimum | 0.95861 | 0.946061 | 0.952898 | 0.943881 | 0.952703 | 0.962167 | 0.911402 | 0.947236 |
| Maximum | 1.045082 | 1.050277 | 1.170643 | 1.04591 | 1.040842 | 1.033631 | 1.027207 | 1.088349 |
| Confidence Level(95.0%) | 0.003462 | 0.003966 | 0.007343 | 0.003623 | 0.003208 | 0.003387 | 0.00407 | 0.004762 |
| | | | | | | | | |
| Lacunarity | | | | | | | | |
| | | | | | | | | |
| Mean | 1.003829 | 1.003472 | 1.008045 | 1.007302 | 1.0141 | 1.00743 | 1.017701 | 1.021988 |
| Standard Error | 0.002433 | 0.00297 | 0.002992 | 0.002693 | 0.00288 | 0.002684 | 0.003217 | 0.002959 |
| Sample Variance | 0.000633 | 0.000917 | 0.000922 | 0.000674 | 0.000788 | 0.000706 | 0.001097 | 0.000823 |
| Minimum | 0.950341 | 0.919244 | 0.938659 | 0.959433 | 0.960272 | 0.921499 | 0.941075 | 0.969537 |
| Maximum | 1.089855 | 1.093819 | 1.084548 | 1.08471 | 1.105387 | 1.083862 | 1.121861 | 1.121861 |
| Confidence Level(95.0%) | 0.004823 | 0.00589 | 0.005934 | 0.005348 | 0.005718 | 0.005327 | 0.00638 | 0.005876 |
| | | | | | | | | |
| Ang. Sec Mom | | | | | | | | |
| | | | | | | | | |
| Mean | 1.043176 | 1.109718 | 1.116278 | 1.058787 | 0.96012 | 1.011229 | 1.093594 | 1.111283 |
| Standard Error | 0.050113 | 0.052768 | 0.062925 | 0.063649 | 0.063607 | 0.070713 | 0.120474 | 0.138382 |
| Sample Variance | 0.045204 | 0.064043 | 0.071271 | 0.093177 | 0.072826 | 0.115007 | 0.261253 | 0.440438 |
| Minimum | 0.658292 | 0.789772 | 0.392 | 0.59431 | 0.44642 | 0.720882 | 0.573806 | 0.392705 |
| Maximum | 1.478809 | 1.89339 | 1.63 | 1.754212 | 1.453253 | 2.016798 | 2.710926 | 3.750436 |
| Confidence Level(95.0%) | 0.10573 | 0.109434 | 0.132759 | 0.132 | 0.1342 | 0.14665 | 0.254179 | 0.286986 |
| | | | | | | | | |
| Mean | | | | | | | | |
| | | | | | | | | |
| Mean | 1.151282 | 1.141222 | 1.110711 | 1.11237 | 1.173554 | 1.178833 | 1.15599 | 1.249105 |
| Standard Error | 0.039466 | 0.038672 | 0.039889 | 0.039622 | 0.046766 | 0.035502 | 0.043136 | 0.040991 |
| Sample Variance | 0.166662 | 0.155534 | 0.163883 | 0.145998 | 0.20777 | 0.123516 | 0.197239 | 0.157948 |
| Minimum | 0.491505 | 0.468247 | 0.373818 | 0.533705 | 0.566094 | 0.504906 | 0.596895 | 0.500813 |
| Maximum | 2.620473 | 2.067474 | 2.461013 | 2.833611 | 2.433622 | 1.976935 | 3.416967 | 2.490574 |
| Confidence Level(95.0%) | 0.078246 | 0.076697 | 0.079119 | 0.078692 | 0.092855 | 0.070461 | 0.085532 | 0.081401 |
| | | | | | | | | |
| Coeff of Variance | | | | | | | | |
| | | | | | | | | |
| Mean | 0.873987 | 0.880154 | 0.808704 | 0.849538 | 0.818386 | 0.830845 | 0.744166 | 0.72828 |
| Standard Error | 0.020556 | 0.028333 | 0.027685 | 0.021841 | 0.027054 | 0.023268 | 0.031038 | 0.032672 |
| Sample Variance | 0.045211 | 0.083486 | 0.078947 | 0.044363 | 0.069532 | 0.053059 | 0.102119 | 0.100343 |
| Minimum | 0.371685 | 0.325561 | 0.296511 | 0.311623 | 0.286104 | 0.265212 | 0.3157 | 0.152894 |
| Maximum | 1.528653 | 1.967861 | 1.861177 | 1.187355 | 1.516266 | 1.397068 | 2.15693 | 1.629918 |
| Confidence Level(95.0%) | 0.040753 | 0.056192 | 0.054914 | 0.043378 | 0.053716 | 0.046181 | 0.061544 | 0.064881 |

are given in table 1 for 5 features. Results of a statistical test on the normality of histograms of the features is presented in table 3, for brevity, results are shown only for five features of the 15 features used for analysis. Since the features of GLDM and SGLDM had similar variations, and, further, since computation of SGLDM features is both time and memory consuming, we discarded the SGLDM features. The features selected are: (i) fractal dimension, (ii) intercept from fractal measures, (iii) lacunarity from fractal measures, (iv) contrast, (v)

**TABLE 2.** Correlation of the features with gestation age.

| | Coef Var | Diff Asm | Diff Con | Diff Ent | Diff Idm | Diff Mean | Entropy | Entropy 1 | Frac Dim | Gestat | Intercept | Kurtosis | Lacunar | Mean | Skew-ness | Variance |
|---|---|---|---|---|---|---|---|---|---|---|---|---|---|---|---|---|
| Coef Var | 1.0000 | -0.2192 | -0.6673 | -0.2259 | -0.0594 | -0.7364 | 0.5818 | -0.7685 | -0.4267 | 0.7800 | -0.5761 | -0.4051 | 0.6935 | -0.1119 | -0.3656 | 0.9776 |
| Diff Asm | -0.2192 | 1.0000 | 0.4350 | 0.9989 | 0.9729 | 0.2437 | -0.5859 | 0.4073 | 0.0960 | -0.6254 | 0.2121 | -0.5351 | -0.7425 | 0.1884 | 0.1079 | -0.1270 |
| Diff Con | -0.6673 | 0.4350 | 1.0000 | 0.4350 | 0.3018 | 0.9670 | -0.5812 | 0.8833 | 0.5760 | -0.8213 | 0.9311 | 0.2865 | -0.7527 | 0.1856 | 0.0125 | -0.6376 |
| Diff Ent | -0.2259 | 0.9989 | 0.4350 | 1.0000 | 0.9734 | 0.2467 | -0.5660 | 0.4050 | 0.0889 | -0.6348 | 0.2221 | -0.5486 | -0.7525 | 0.2214 | 0.0852 | -0.1358 |
| Diff Idm | -0.0594 | 0.9729 | 0.3018 | 0.9734 | 1.0000 | 0.0941 | -0.4183 | 0.2038 | 0.1141 | -0.5195 | 0.1022 | -0.7073 | -0.6091 | 0.2298 | 0.0756 | 0.0527 |
| Diff Mean | -0.7364 | 0.2437 | 0.9670 | 0.2467 | 0.0941 | 1.0000 | -0.5054 | 0.8800 | 0.5850 | -0.7780 | 0.9579 | 0.4437 | -0.6869 | 0.1902 | -0.0585 | -0.7431 |
| Entropy | 0.5818 | -0.5859 | -0.5812 | -0.5660 | -0.4183 | -0.5054 | 1.0000 | -0.7642 | -0.1149 | 0.4937 | -0.3432 | -0.2921 | 0.6029 | 0.4462 | -0.4580 | 0.5471 |
| Entropy 1 | -0.7685 | 0.4073 | 0.8833 | 0.4050 | 0.2038 | 0.8800 | -0.7642 | 1.0000 | 0.2321 | -0.7620 | 0.7607 | 0.4955 | -0.8116 | 0.0442 | 0.1218 | -0.7868 |
| Frac Dim | -0.4267 | 0.0960 | 0.5760 | 0.0889 | 0.1141 | 0.5850 | -0.1149 | 0.2321 | 1.0000 | -0.5010 | 0.5781 | 0.0138 | -0.1978 | 0.0886 | 0.1526 | -0.3263 |
| Gestat | 0.7800 | -0.6254 | -0.8213 | -0.6348 | -0.5195 | -0.7780 | 0.4937 | -0.7620 | -0.5010 | 1.0000 | -0.6856 | 0.0281 | 0.9358 | -0.4939 | -0.1108 | 0.7207 |
| Intercept | -0.5761 | 0.2121 | 0.9311 | 0.2221 | 0.1022 | 0.9579 | -0.3432 | 0.7607 | 0.5781 | -0.6856 | 1.0000 | 0.3203 | -0.5923 | 0.2650 | -0.2552 | -0.5897 |
| Kurtosis | -0.4051 | -0.5351 | 0.2865 | -0.5486 | -0.7073 | 0.4437 | -0.2921 | 0.4955 | 0.0138 | 0.0281 | 0.3203 | 1.0000 | 0.0420 | -0.3917 | 0.1322 | -0.5102 |
| Lacunar | 0.6935 | -0.7425 | -0.7527 | -0.7525 | -0.6091 | -0.6869 | 0.6029 | -0.8116 | -0.1978 | 0.9358 | -0.5923 | 0.0420 | 1.0000 | -0.4445 | -0.0326 | 0.6683 |
| Mean | -0.1119 | 0.1884 | 0.1856 | 0.2214 | 0.2298 | 0.1902 | 0.4462 | 0.0442 | 0.0886 | -0.4939 | 0.2650 | -0.3917 | -0.4445 | 1.0000 | -0.4651 | -0.1185 |
| Skew-ness | -0.3656 | 0.1079 | 0.0125 | 0.0852 | 0.0756 | -0.0585 | -0.4580 | 0.1218 | 0.1526 | -0.1108 | -0.2552 | 0.1322 | -0.0326 | -0.4651 | 1.0000 | -0.2247 |
| Variance | 0.9776 | -0.1270 | -0.6376 | -0.1358 | 0.0527 | -0.7431 | 0.5471 | -0.7868 | -0.3263 | 0.7207 | -0.5897 | -0.5102 | 0.6683 | -0.1185 | -0.2247 | 1.0000 |

**TABLE 3.** Normal distribution parameters of the features.

| Gestation Age | | 24 | 26 | 28 | 30 | 32 | 34 | 36 | 38 |
|---|---|---|---|---|---|---|---|---|---|
| Features | | | | | | | | | |
| Fractal Dimension | muhat | 1.0006 | 0.9902 | 0.9987 | 0.9955 | 0.9956 | 0.9963 | 0.9824 | 0.9923 |
| | sigmahat | 0.0143 | 0.0270 | 0.0214 | 0.0154 | 0.0152 | 0.0154 | 0.0191 | 0.0267 |
| | | | | | | | | | |
| | mu confidence int | 0.9933 | 0.9764 | 0.9878 | 0.9876 | 0.9878 | 0.9884 | 0.9726 | 0.9787 |
| | | 1.0080 | 1.0040 | 1.0097 | 1.0034 | 1.0034 | 1.0042 | 0.9921 | 1.0060 |
| | | | | | | | | | |
| | sigma confidence int | 0.0107 | 0.0202 | 0.0161 | 0.0116 | 0.0114 | 0.0115 | 0.0143 | 0.0200 |
| | | 0.0215 | 0.0404 | 0.0321 | 0.0231 | 0.0228 | 0.0230 | 0.0286 | 0.0401 |
| | | | | | | | | | |
| | | | | | | | | | |
| lacunarity | muhat | 1.0032 | 0.9949 | 1.0061 | 1.0050 | 1.0129 | 1.0222 | 1.0145 | 1.0210 |
| | sigmahat | 0.0297 | 0.0320 | 0.0304 | 0.0270 | 0.0271 | 0.0262 | 0.0271 | 0.0285 |
| | | | | | | | | | |
| | mu confidence int | 0.9880 | 0.9786 | 0.9905 | 0.9912 | 0.9990 | 1.0089 | 1.0006 | 1.0064 |
| | | 1.0184 | 1.0113 | 1.0216 | 1.0189 | 1.0268 | 1.0356 | 1.0283 | 1.0356 |
| | | | | | | | | | |
| | sigma confidence int | 0.0223 | 0.0240 | 0.0228 | 0.0203 | 0.0204 | 0.0196 | 0.0204 | 0.0214 |
| | | 0.0445 | 0.0480 | 0.0456 | 0.0405 | 0.0407 | 0.0392 | 0.0407 | 0.0428 |
| | | | | | | | | | |
| | | | | | | | | | |
| Ang sec mom | muhat | 1.0400 | 1.1100 | 1.1200 | 1.0900 | 0.9600 | 0.9800 | 1.0900 | 1.1500 |
| | sigmahat | 0.2130 | 0.2490 | 0.2670 | 0.3250 | 0.2700 | 0.3250 | 0.5110 | 0.7120 |
| | | | | | | | | | |
| | mu confidence int | 0.9340 | 0.9870 | 0.9790 | 0.9230 | 0.8220 | 0.8140 | 0.8320 | 0.7820 |
| | | 1.1500 | 1.2400 | 1.2500 | 1.2600 | 1.1000 | 1.1500 | 1.3600 | 1.5100 |
| | | | | | | | | | |
| | sigma confidence int | 0.1600 | 0.1870 | 0.2000 | 0.2440 | 0.2030 | 0.2440 | 0.3840 | 0.5340 |
| | | 0.3190 | 0.3730 | 0.4000 | 0.4880 | 0.4050 | 0.4870 | 0.7660 | 1.0700 |
| | | | | | | | | | |
| | | | | | | | | | |
| Mean | muhat | 1.0000 | 1.0000 | 0.9990 | 1.0000 | 0.9980 | 1.0000 | 0.9990 | 0.9980 |
| | sigmahat | 0.0053 | 0.0061 | 0.0043 | 0.0050 | 0.0065 | 0.0058 | 0.0060 | 0.0074 |
| | | | | | | | | | |
| | mu confidence int | 0.9970 | 0.9970 | 0.9960 | 0.9980 | 0.9950 | 0.9970 | 0.9950 | 0.9940 |
| | | 1.0000 | 1.0000 | 1.0000 | 1.0000 | 1.0000 | 1.0000 | 1.0000 | 1.0000 |
| | | | | | | | | | |
| | sigma confidence int | 0.0040 | 0.0045 | 0.0033 | 0.0038 | 0.0049 | 0.0043 | 0.0045 | 0.0056 |
| | | 0.0079 | 0.0091 | 0.0065 | 0.0076 | 0.0097 | 0.0087 | 0.0090 | 0.0111 |
| | | | | | | | | | |
| Variance | muhat | 1.2500 | 1.2900 | 1.3600 | 1.6300 | 1.6300 | 1.5000 | 1.4700 | 1.6100 |
| | sigmahat | 0.8530 | 0.7190 | 0.9120 | 1.1600 | 1.5700 | 0.6950 | 0.9570 | 0.8560 |
| | | | | | | | | | |
| | mu confidence int | 0.8130 | 0.9270 | 0.8980 | 1.0400 | 0.8240 | 1.1500 | 0.9750 | 1.1700 |
| | | 1.6900 | 1.6600 | 1.8300 | 2.2300 | 2.4300 | 1.8600 | 1.9500 | 2.0500 |
| | | | | | | | | | |
| | sigma confidence int | 0.6400 | 0.5400 | 0.6840 | 0.8710 | 1.1800 | 0.5220 | 0.7180 | 0.6420 |
| | | 1.2800 | 1.0800 | 1.3700 | 1.7400 | 2.3500 | 1.0400 | 1.4300 | 1.2800 |

angular second moment, (vi) entropy, (vii) mean from GLDM, (viii) inverse difference moment from GLDM, (ix) entropy measures from the $L5^TE5$ mask, (x) entropy measures from the $L5^TS5$ mask, (xi) mean from the histogram of the image, (xii) variance from the histogram, (xiii) coefficient of variation from the histogram, (xiv) skewness of the histogram, and (xv) kurtosis of the histogram. It is observed that data sets from both the hospitals exhibit similar behavior. Figure 1 illustrates the variation of the mean features with respect to the gestation age. The variable plotted is the mean of the ratios of the value of lung to liver feature. The experimental data has been fitted with a second degree polynomial based on least square error. The variation of only six of the above 15 features are shown in figure 1. We can see that parameters, fractal dimension, lacunarity from fractal measures, angular second moment from GLDM, mean echogenicity, variance from the histogram and coefficient of variation from the histogram have trends that could possibly have some predictive value.

Figure 2 demonstrates the dynamics of the chosen features as a function of the gestation age for the lung and the liver. Figures 2(a) and (b) show that the fractal dimension and lacunarity increase as a function of the gestation age. Figure 2(d) shows a decrease in the echogenicity of lung as compared to the liver as the gestation age increases. The echogenicity of the lung is almost the same as the echogenicity of the liver at early gestation age. Thus, the lung seems to attenuate ultrasound waves more than the liver at later gestation ages (cf. reference [4]). The variance of the gray values of the lung (Fig. 2(e)) has an upward trend whereas that of the liver remains almost at the same level.

As seen from figure 2, the nature of variation of the features of the liver is, in most cases, similar to that of the lung. In the case of the other parameters also, the liver shows lot of change as a function of the gestation age. Since the tissues imaged are at the same depth for both the lung and the liver, the features, which are mainly textural in nature, are reasonably insensitive to the settings of the imaging system. This questions one of the basic assumptions, namely, that the sonographic features of the liver are expected to remain constant, starting from the gestation age of 24 weeks, and thus can be taken as a reference. The conclusions of majority of the previous investigators are based on the study of only the echogenicity of the liver and lung, which are more sensitive to the imaging parameters than the textural features.

## 4. CONCLUSIONS

The ultrasound image formation depends on many factors. Hence, we have tried to maintain most of the machine parameters at a constant value. Since all the subjects studied are normal, large variations in depth were not encountered in the study. Moreover, the lung and liver areas taken for analysis were contiguous and at the same depth for each fetus. Since in all the cases, the lung and the liver have been imaged together, the effects due to the imaging techniques (including the internal processing by the machine) could be expected to affect both the regions similarly. Thus, the ratios of the textural features are better indicators of the histological changes, compared to the study of only the echogenicity. Further, some of the features studied show some notable trend. Based on the data analyzed, it appears that the characteristics of the ultrasound images hold promise in the analysis of the maturity of the fetal lung. Thus, a complete sonographic analysis, which combines the above textural features with parameters such as fetal biparietal diameter, placental grading, femur length, head circumference and the abdominal circumference could possibly enhance the prediction accuracy. Also, an analysis of data from high-risk pregnancies (mothers with hypertension or

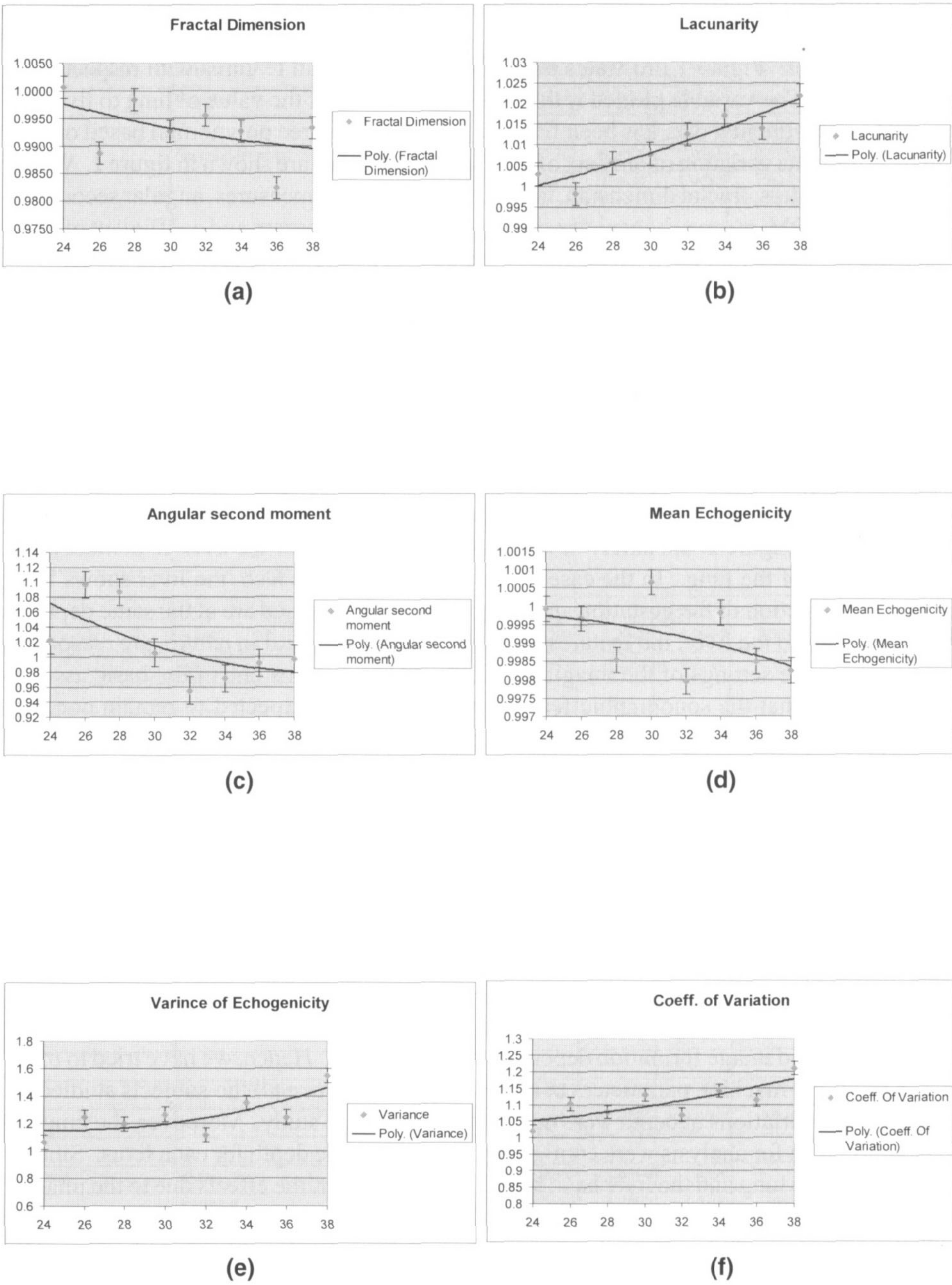


**FIG. 1** Plot showing the variation of means of the ratios of lung to liver feature values with respect to the gestation age. The curve shown is a least square fit of the points by a second degree polynomial. Top row: ( a): fractal dimension, (b): lacunarity. Second row: (c): angular second moment, (d): mean calculated from the histogram of the image. Bottom row : (e): variance obtained from the histogram, (f): coefficient of variation computed from the histogram.

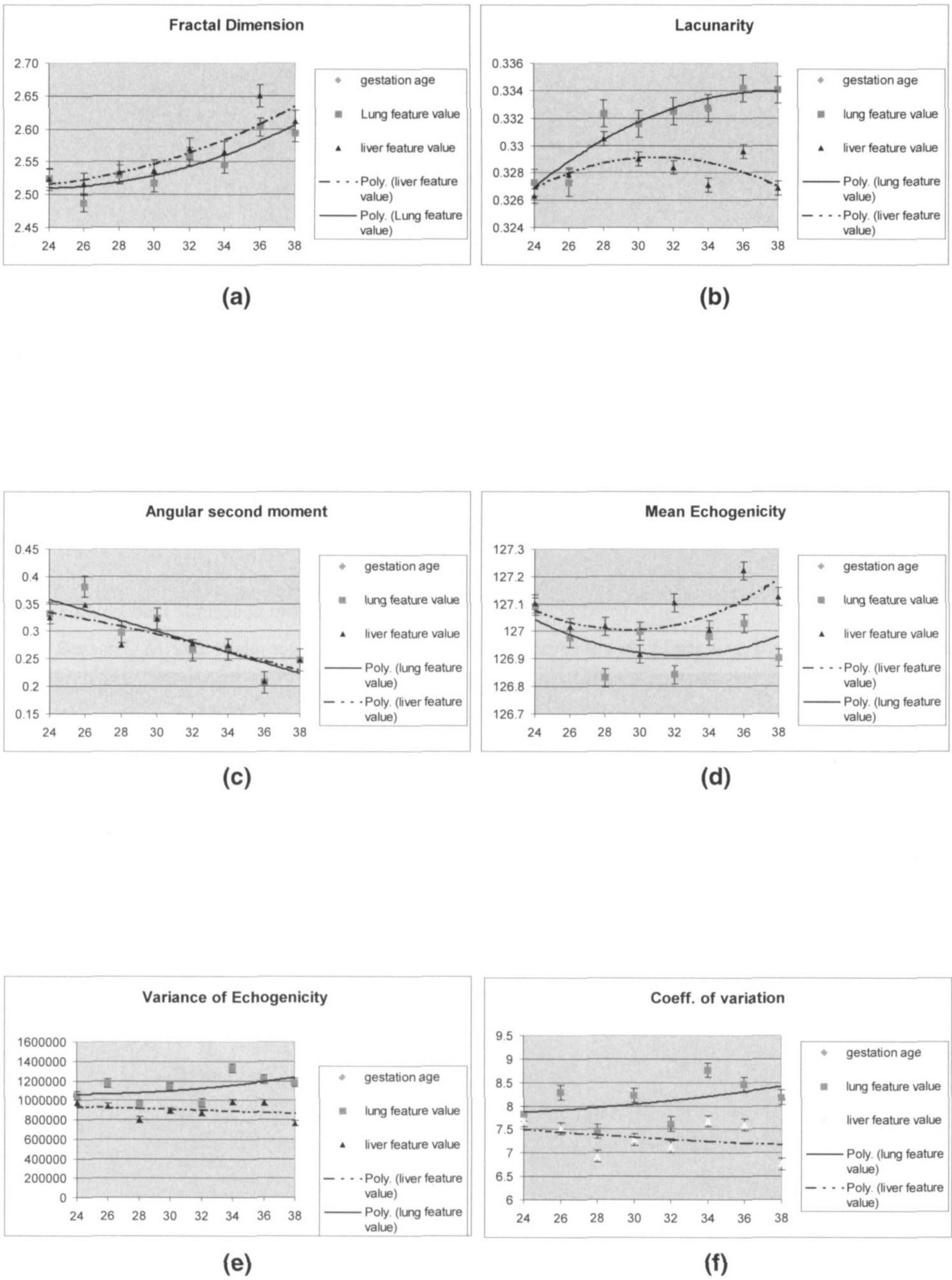


**FIG. 2** Plot showing the variation of the mean of various features of lung and liver with respect to the gestation age. The curves shown are the least square fits of the points by second degree polynomials. Top row: ( a): fractal dimension, (b): lacunarity. Second row: (c): angular second moment, (d): mean calculated from the histogram of the image. Bottom row : (e): variance obtained from the histogram, (f): coefficient of variation calculated from the histogram.

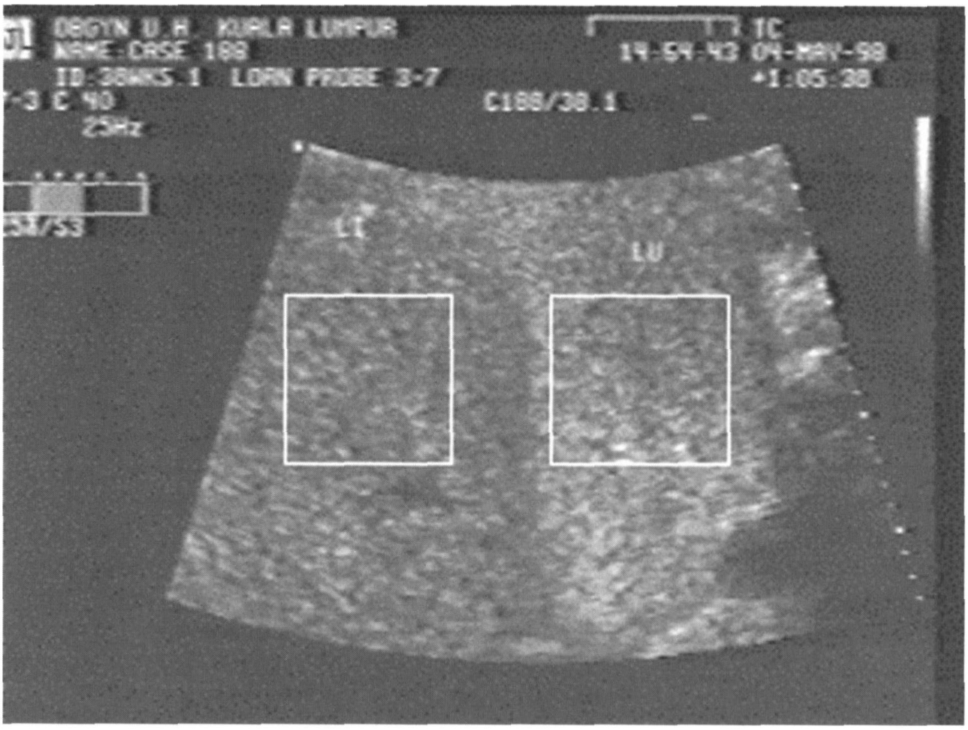


(a)

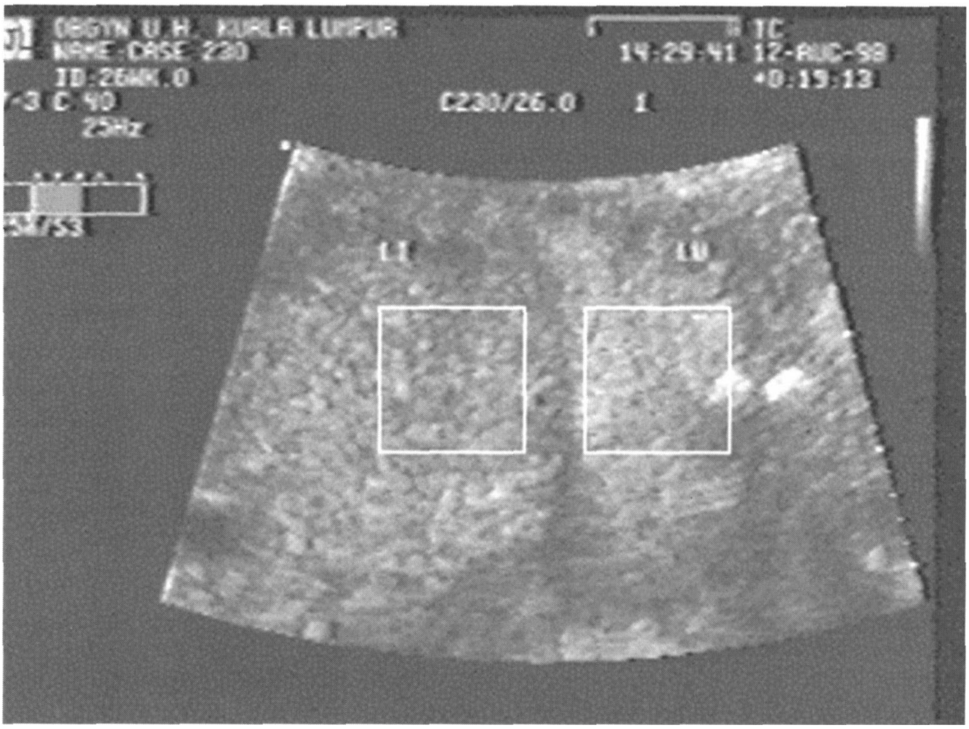


(b)

**FIG. 3** Sample fetal echogram images showing the regions of liver and lung.

diabetes mellitus) could be used to further validate the prediction of maturity using sonographic features.

## 5. ACKNOWLEDGMENTS

We are thankful to Dr. Subbukrishna, Associate Professor, Department of Biostatistics, NIMHANS, Bangalore, for his valuable suggestions and helping us in analyzing the data. We thank the anonymous reviewers for their valuable suggestions and comments.

## REFERENCES

1. Charnock, E.L. and Doershuk, C.F., Developmental aspects of the human lung, *Pediatr. Clin. N. Amer., 20,* 275-292 (1973).

2. Feingold, M., Scollins, J., Cetrulo, C. and Koza, D., Fetal lung to liver reflectivity ratio and lung maturity, *J. Clin. Ultrasound 15,* 384-387 (1987).

3. Thieme, G. A., Banjavic, R. A., Johnson, et al, Sonographic identification of lung maturation in the fetal lamb, *Invest. Radiol. 18,* 18 -26 (1983).

4. Garrett, W.J., Warren, P.S. and Picker, R.H., Maturation of the fetal lung, liver, and bowel, in *Proc. Am. Inst. Ultras. Med.,* p. 93 (1980)(abstract).

5. Cayea P.D., Grant D.C., Doubilet P.M. and Jones.T.B., Prediction of fetal lung maturity: inaccuracy of study using conventional ultrasound instruments, *Radiol. 155,* 473-475 (1985).

6. Benson D.M. and. Waldroup L.D., Ultrasonic tissue characterization of fetal lung, liver and placenta for the purpose of assessing fetal maturity, *J. Ultras. Med. 2,* 489-494 (1983).

7. Podobnik, M., Brayer, B. and Ciglar, B., Ultrasonic fetal and placenta tissue characterization and lung maturity, *Int. J. Gyn. Obstet. 54,* 221-229 (1996).

8. Carson, P. L., Meyer, C.R., Bowerman, R.A., Bland, P.H. and Bookstein, F.L., Prediction of pulmonary maturity from ultrasound scattering, in *Tissue Characterization with Ultrasound,* J.F. Greenleaf, Ed., pp. 169-187 (CRC Press, Boca Raton, FL, 1986).

9. Carson, P. L., Meyer, C. R. and Bowerman, R. A., Prediction of fetal lung maturity with ultrasound, *Radiol. 155,* 533 (1985).

10. Sohn, C., Stolz, W., Gast, A.S. and Basert, G., Ultrasound diagnosis of fetal lung maturity, *Zentralbl Geburtshilfe Perinatol. 196,* 55-60 (1992).

11. Gast, A.S., Sohn, C. and Basert, G., Ultrasound diagnosis of fetal lung maturity, Zentralbl Gynak*ol 117,* 138-143(1995).

12. Christie, A.D., *Determination of fetal lung development by ultrasound image analysis,* Technical Report (Ninewell's Hospital, Scotland, 1992).

13. Haralick, R.M., Statistical and structural approaches to texture, *Proc. IEEE 67,* 304-322 (1979).

14. Conners R.W. and Harlow C.A., A theoretical comparison of texture algorithms, *IEEE Trans. PAMI 2,* 204-222 (1980).

15. Valckx, F.M. and Thijssen, J.M., Characterization of echographic image texture by cooccurrence matrix parameters, *Ultrasound Med. Biol. 23,* 559-571 (1997).

16. Raeth, U., Schlaps, D., Limberg, B., Zuna, I., Van Kaick, G., Lorenz, W.J. and Kommerell, B., Diagnostic accuracy of computerized B-scan texture analysis and conventional ultrasonography in diffuse parenchymal and malignant liver disease, *J. Clin.Ultras.13,* 87-99 (1985).

17. Chen, C.C., Daponte, J.S. and Fox, M.D., Fractal feature analysis and classification in medical imaging, *IEEE Trans. Med. Imaging 8,* 133-142 (1989).

18. Verhoeven, J.T. and Thijssen, J. M., Potential of fractal analysis for lesion detection in echographic images, *Ultrasonic Imaging, 15,* 304-323(1993); Laws, K.I., Texture energy measures, in *Proc. Image Understanding Workshop,* pp. 47-51 (1979).

19. Keller J.M., Chen S., and Crownover, Texture description and segmentation through fractal geometry, *Comp. Vision Graphics Image Proc. 45,* 150-166 (1989).

20. Laws, K. I., Texture energy measures, in *Proc. Image Understanding Workshop,* pp. 47-51 (1979).

21. Bhanu Prakash K.N, Suresh, S. and Ramakrishnan. A.G, Can sonogram predict fetal lung maturity?, *Crit. Rev. Biomed. Engin. 26,* 350-351 (1998).

22. Bhanu Prakash K.N., Ramakrishnan A.G., Suresh, S. and Chow, W.P., Fetal lung maturity analysis using sonogram textural features, in *Proc. Symp. Biomed. Engin.-2000,* BARC, Mumbai, India, pp. 155 –158 (2000).

23. Weszka J.S., Dyer C.R., and Rosenfeld A.A comparative study of texture measures for terrain classification, *IEEE Trans. Syst. Man Cybern. SMC-6,* 269-285 (1976).